Single grain optically stimulated luminescence dating of glacial sediments from the Baiyu Valley, southeastern Tibet

Ou, Xianjiao; Duller, G. A. T.; Roberts, H. M.; Zhou, ShangZhe; Lai, Z. P.; Chen, Rong; Chen, RenRong; Zeng, Lanhua

Published in:
Quaternary Geochronology

DOI:
10.1016/j.quageo.2015.02.018

Publication date:
2015

Citation for published version (APA):
Ou, X., Duller, G. A. T., Roberts, H. M., Zhou, S., Lai, Z. P., Chen, R., Chen, R., & Zeng, L. (2015). Single grain optically stimulated luminescence dating of glacial sediments from the Baiyu Valley, southeastern Tibet. *Quaternary Geochronology*, *30*(B), 314-319. https://doi.org/10.1016/j.quageo.2015.02.018

Published in Quaternary Geochronology (2015) – DOI: 10.1016/j.quageo.2015.02.018

Single grain optically stimulated luminescence dating of glacial sediments from the Baiyu Valley, southeastern Tibet

XianJiao Ou[1,2*], Geoff A.T. Duller[2], Helen M. Roberts[2], ShangZhe Zhou[3], ZhongPing Lai[4], Rong Chen[5], RenRong Chen[3], LanHua Zeng[1]

[1] *School of Geography and Tourism, Jiaying University, Meizhou 514015, China*
[2] *Department of Geography and Earth Sciences, Aberystwyth University, Ceredigion SY23 3DB, UK*
[3] *School of Geographical Science, South China Normal University, Guangzhou 510631, China*
[4] *School of Earth Sciences, China University of Geosciences, Wuhan 430074, China*
[5] *Nanjing Institute of Geography and Limnology, Chinese Academy of Sciences, Nanjing 210008, China*

Abstract: The Qinghai-Tibetan Plateau is an important area for the study of Quaternary glaciation. Optically stimulated luminescence (OSL) dating has the potential to contribute to the chronology of glaciation in this region, but it is important to assess the accuracy of OSL dating of these glacial sediments. In this study, single grain quartz OSL signals are examined for five glacial samples collected from the moraines outside the Baiyu Valley, southeastern Tibet. The quartz grains exhibit poor luminescence characteristics, with a small proportion of grains passing the screening criteria. Grains which pass the screening criteria have relatively low signal intensity, leading to D_e values with large uncertainties. MAM and CAM were used to determine D_e values for these samples. The OSL ages are consistent with the sequence of events derived from the geomorphological relationship of the samples, and also with previous published radiocarbon ages. However, it is more difficult to reconcile the OSL ages and the terrestrial cosmogenic nuclide (TCN) ^{10}Be ages. Analysis of both single grain quartz OSL data and TCN ^{10}Be data is complex in this area. Further work is required to increase confidence in the OSL ages generated for the glacial sediments from this region.

Key words: Incomplete bleaching; minimum age model; OSL; quartz; moraine; till; glaciofluvial sediments; Nyainqentanglha Range; Qinghai-Tibetan Plateau

1. Introduction

The Qinghai-Tibetan Plateau has a profound influence on regional and global atmospheric circulation, and is therefore important for understanding the dynamics of global environmental change. The plateau and the surrounding mountains are the most glaciated region beyond the polar realm, and provide excellent archives for the reconstruction of palaeoglaciation, which is of critical importance for understanding palaeoclimatic change. However, the timing of glacier fluctuations in this region remains controversial. Optically stimulated luminescence (OSL) dating is one of the few techniques that can potentially provide a chronology for glacial sediments. However, dating glacial sediments is difficult, not least because the OSL signal is often not fully bleached prior to deposition of

* Corresponding author. Phone: +86(0)13727608114.
E-mail address: ouxianjiao@163.com (X-J. Ou)

the sediments; additionally, signal levels are frequently reported to be dim for quartz in glacial settings (e.g. Richards et al., 2000).

There have been several previous OSL studies in this region over the last decade. With the exception of one sample (considered in Owen et al., 2009), these studies were based on multiple grain measurements. Most studies used large aliquots for dating (Richards et al., 2000; Tsukamoto et al., 2002; Spencer and Owen, 2004; Owen et al., 2009; Xu et al., 2009; Zhang et al., 2012; Zhao et al., 2012; Ou et al., 2014; 2015). Only a small number of OSL ages were obtained using small aliquots (~3 mm aliquots (Chen et al., 2014); 2 mm aliquots (Hu et al., 2014); 1 mm aliquots (Rhodes and Bailey, 1997)). Large residual doses (up to ~100-200 Gy) were reported for some of the young and modern samples examined from this region (Ou et al., 2014; 2015). However, as these samples were dated by large aliquots containing many thousands of grains it was not possible to investigate whether these samples also contained a population of well-bleached grains (Ou et al., 2014; 2015).

The OSL signal of few glacial samples is uniformly reset on deposition. Multiple grain aliquots comprising large numbers of grains that give light cannot be used to assess the degree of incomplete bleaching as it is likely to be obscured by the effects of averaging between grains (Duller, 2008). There could be significant age overestimation if incompletely bleached samples are measured using multiple grain aliquots (Duller, 2006). In contrast, single grain, and potentially small aliquot, methods offer the potential for identifying the well-bleached grains from glacial sediments.

In this study, single grain OSL ages are determined for glacial sediments from the Baiyu Valley in southeastern Tibet. The site benefits from having independent dating evidence, including terrestrial cosmogenic nuclide (TCN) Beryllium-10 (^{10}Be) and radiocarbon (^{14}C) ages (Zhou et al., 2007; 2010). This study explores the application of single grain OSL methods to glacial sediments from the Qinghai-Tibetan Plateau and the surrounding mountains.

2. Materials and methods

2.1 Study area and sample locations

The study area is located in the eastern Nyainqentanglha Mountains, southeastern Tibet (Fig.1a), close to the 'Grand Canyon' and 'Great Bend' of the Yarlung Zangbo River, which is the upper course of the Brahmaputra River. The Baiyu Valley is a tributary valley of the Bodui Zangbo River, which in turn is a tributary river of the Parlung Zangbo River (Fig.1b), which is itself a main tributary river of the Yarlung Zangbo River. Southeastern Tibet is heavily influenced by the Indian Monsoon, receiving the highest precipitation on the Qinghai-Tibetan Plateau (annual precipitation near the equilibrium line altitude is ~3000 mm), and is typical of the region of monsoonal maritime glaciers in China. Two well-known regional glacial stages in China, the Guxiang and Baiyu glaciations, were proposed in and named after this area (Li et al., 1986). The Baiyu glaciation itself was named after the associated moraines that reached Baiyu Village (located ~1 km west of the Baiyu Valley) in the Bodui Zangbo Valley. Outside the Baiyu Valley, well-preserved prominent lateral moraines (30°05'N, 95°31'E) with multiple crests reach heights of 100−200 m above the valley floor (~2900 m asl), and were also attributed to the Baiyu glaciation (Li et al., 1986). Five OSL samples were collected from these moraines (Fig.1c); Aber/213-BY202, -BY203 and -BY301 are till samples comprised of clast-rich diamictons, collected into a bag under a blackout tarpaulin, whilst Aber/213-BY201 and -BY302 are glaciofluvial samples collected by hammering metal tubes into sand lenses interbedded within the moraines.

2.2 Sample preparation

Samples were treated with a 10% v.v. dilution of concentrated (37%) hydrochloric acid (HCl) to remove carbonates, followed by 20 vols. (~6%) hydrogen peroxide (H_2O_2) to remove organics. Samples were dry-sieved, prior to density separation of the 90−150 μm diameter fraction of sample BY302, and the 180−210 μm diameter fraction of the remaining four samples, using sodium polytungstate to isolate the quartz-rich fraction. Samples were etched in 40% hydrofluoric (HF) acid for 45 min to remove feldspars and the outer alpha-irradiated portion of the quartz grains, followed by washing with concentrated HCl for 45 min to remove insoluble fluorides. The remaining grains were then re-sieved to purify the quartz-rich fraction, prior to use for OSL measurement.

2.3 Equipment and optically stimulated luminescence measurements

OSL measurements were carried out using a Risø TL-DA-15 reader equipped with a single grain luminescence system based around a 10 mW Nd:YVO_4 laser emitting at 532 nm, with a power density of ~50 W/cm^2. Photon detection was achieved using an EMI 9235QA photo-multiplier filtered by 2 mm of Schott BG-39, and 2.5 mm of Hoya U-340 filter, and a convex quartz lens to enhance the signal collection efficiency. A ^{90}Sr/^{90}Y beta source delivering 5.15 Gy/min to the grains was used for irradiation.

All measurements were conducted using a single aliquot regenerative dose (SAR) (Murray and Wintle, 2000) procedure employing a preheat of 220 ^{o}C (heated at 5 ^{o}C/s) for 10 s prior to measurement of the natural or regenerative signal (L_x), and a preheat of 160 ^{o}C (heated at 5 ^{o}C/s) with immediate cooling prior to the measurement of the response to a test dose (T_x). The duration of optical stimulation was 1 s at a temperature of 125 ^{o}C (heated at 5 ^{o}C/s). The L_x and T_x signals used for dating were derived from the first 0.17 s of the OSL signal minus a mean background count for the last 0.25 s of the decay curve.

Environmental dose rates were assessed in the laboratory from thick source alpha- and beta-counting, using Daybreak™ alpha counters and a Risø GM-25-5 beta counter. No portable gamma spectrometer was available for use in the field. The coarse-grain quartz dose rates calculated are shown in Table S1.

3. Results

3.1 OSL signal characteristics and dose recovery tests

To characterize the OSL signal and test the suitability of the SAR measurement protocol to be used for dating, single-grain dose recovery tests were conducted using unheated aliquots of samples BY201 and BY202. The natural OSL signal from 500 grains of BY201 and 4000 grains from BY202 were bleached twice with the green laser in the single grain system for 1 s at 30 ^{o}C, with a 10,000 s pause between these bleaches to allow any charge within the 110 ^{o}C trap to be emptied. A beta dose of 68.8 Gy was then given, prior to application of the SAR measurement protocol described in section 2.3 to assess the ability to recover this known dose. The single-grain data generated throughout this study were screened according to a number of quality control criteria, namely: (1) recycling ratio within 10% of unity, (2) OSL IR depletion ratio within 10% of unity (Duller, 2003), (3) maximum uncertainty in T_x less than 20%, and (4) OSL signal greater than 3 σ above background. Only grains that passed all of these screening criteria were used for the determination of either the laboratory-given dose or the natural D_e value.

Unlike many published studies of glacial sediments using coarse-grained quartz (e.g. Duller, 2006), a relatively high proportion of the grains examined gave a discernible OSL signal (15%), but in spite of the fact that many of these grains gave dose response curves (e.g. Fig 2a), the majority failed the OSL IR depletion ratio test, and after application of this criteria only 0.85% of the total measured grains were accepted. Given the careful sample preparation that was undertaken, designed to isolate quartz grains and exclude feldspars, the existence of this large number of grains that are sensitive to IR is surprising. Visual inspection of the grains, and ongoing experiments to explore the nature of these grains, imply that the IR sensitive grains are indeed quartz, but further work is needed to confirm this. At present we have taken a cautious approach and excluded all grains that fail the OSL IR depletion ratio test. Those grains that passed all screening criteria tended to be dimmer than those grains that failed the OSL IR depletion ratio (cf Figs 2a and b), and they contribute a very low proportion of the total available light summed from all grains measured in the dose recovery tests e.g. from 4000 single grains measured for sample BY202, only 0.8 % of the total light is derived from grains that pass all the quality control checks. These observations highlight the need for a single-grain approach for dating these samples because multiple grain aliquots of any size would almost certainly fail the screening criteria (particularly the OSL IR depletion ratio test); this assertion was confirmed by the vast majority of aliquots failing the OSL IR depletion ratio criterion when single grain data were combined to create synthetic aliquots.

For sample BY201, 11 grains from the 500 measured gave dose values, and produced a dose recovery ratio of 0.92 ± 0.11 with an overdispersion of 30%. For sample BY202 where a greater amount of material was available, 34 grains from the 4000 measured yielded dose values (Fig. 2c). The ratio of the recovered dose 77.6 ± 5.0 Gy to the given dose is 1.13 ± 0.07, and overdispersion (OD) is 27%. These values imply that there is a large degree of natural variability in the behaviour of the grains within each sample, even after stringent screening tests for quality control; this variability in behaviour will underlie any additional variability arising from inhomogeneous bleaching of the OSL signal prior to deposition.

3.2 Single grain equivalent dose distributions

To determine the laboratory equivalent dose (D_e) for the natural OSL signal, between 2100 and 4500 grains were measured for each of the five samples using the same SAR protocol used for the dose recovery tests (Table 1). As noted for the dose recovery tests, and reported in other studies (e.g. Duller, 2006), a large proportion of the grains failed the acceptance criteria. Within those grains that gave OSL signals, between 63 to 98 % failed the OSL IR depletion ratio test, demonstrating that the material separated as quartz contains a high proportion of grains that are sensitive to infrared. As noted for the dose recovery dataset, most of the grains that pass all the criteria are dim grains and exhibit large uncertainties (e.g. Fig. 2b), while many grains that pass criteria 1, 3 and 4 but fail the OSL IR depletion ratio show relatively small uncertainties (Fig. 2a).

For sample BY203, only nine grains out of 3800 grains measured (0.24 %) passed all of the screening criteria, which made it impractical to obtain sufficient data for further analysis. For the remaining four samples, between 49 and 96 grains (1.1 % to 4.6% of the total number measured) were accepted following application of the screening criteria, and used to define the D_e distributions (Fig. 3 and S1). The OD values for BY201, 202, 203 and 301 range from 73−93% (Table 1) and the D_e distributions are asymmetric. Therefore the minimum age model (MAM) (Galbraith et al., 1999) has been used to calculate the D_e (Table 1). As the OD of the two dose recovery tests was high (30 % and 27 %), a high sigma b value of 0.4 was used when running the minimum age model. Sample BY302 (Fig 3b) has OD lower than the other samples (55%), and given the high OD seen in the dose recovery data (Fig 2c) the central age model has been applied to this data set (Table 1).

4. OSL ages and comparison with independent ages

The samples dated using single grain OSL techniques were collected from different moraine ridges (Fig. 1c). According to the geomorphology, samples BY201 and BY202 are expected to be similar in age, and younger than either samples BY301 or BY302. Sample BY301 is older than sample BY302, based on the geomorphology, although the time interval between the deposition of the moraine ridges from which these samples were taken may be too short to be resolved using OSL dating. The OSL ages shown in Table 1 range from 14.4 ± 4.2 ka (BY301) to 7.95 ± 2.47 ka (BY202) and have relatively large uncertainties. The oldest and the youngest ages agree within 1σ uncertainties; nevertheless, it is interesting to note that the central values for the four OSL ages are consistent with the geomorphic model of deposition i.e. sample BY301 (14.4 ± 4.2 ka) is older than sample BY302 (11.3 ± 1.0 ka), which in turn is older than samples BY201 and BY202, which are themselves likely to be of similar age (9.43 ± 2.72 and 7.95 ± 2.47 ka, respectively).

Some independent constraints on the likely timing of this sequence of depositional events is offered by radiocarbon and terrestrial cosmogenic nuclide (TCN) ages presented in Zhou et al. (2007; 2010). Radiocarbon ages have been published for moraines containing two palaeosols, the lowermost of which contained charcoal which may have been associated with a warmer Holocene climatic optimum (Zhou et al., 2010). These upper and lower buried soils, dated to 2.60 ± 0.16 and 7.14 ± 0.18 cal ka BP respectively (Zhou et al., 2010), serve as minimum ages for the deposition of the moraine ridges into which these later soils are developed. The OSL ages generated are all older than these radiocarbon minimum ages, and hence these two lines of dating evidence are consistent with each other.

The cosmogenic ^{10}Be ages of the nine boulders (1−2 boulders per moraine ridge) from the Baiyu Valley presented in (Zhou et al., 2007) were recalculated using the Lal (1991)−Stone (2000) time-dependent model applying the latest reported ^{10}Be half-life of 1.387 Ma (Chmeleff et al., 2010; Korschinek et al., 2010). Discounting an obvious young outlier, these TCN ages range from 11.0 ± 0.9 to 21.1 ± 1.8 ka (Fig. 1c). The single grain OSL ages all agree within errors with the lower-end of this TCN age range. However, it is possible that the ^{10}Be ages are underestimates due to high precipitation in this region causing erosion of the boulder surface. Furthermore, many authors have argued that exposure ages on moraines are more likely to have a young bias due to exhumation, boulder rotation, shielding, rock-surface erosion and weathering, etc (Balco, 2011). Whilst prior exposure (inheritance) would give older boulder ages, incomplete exposure is considered to be more common than prior exposure, and thus the oldest, rather than either the youngest or even the average age best represents the age of the moraine (Putkonen and Swanson, 2003; Balco, 2011; Heyman et al., 2011). If this holds true for the moraines outside the Baiyu Valley, the upper end of the ^{10}Be age range (21.1 ± 1.8 ka) in Fig. 1c is more likely to reflect the age of the moraine, which then enlarges the discrepancy between the ^{10}Be and OSL ages. Some offset between the OSL and TCN ages may be expected because the OSL age reflects the time of deposition of glacial or glaciofluvial sediments, whilst the TCN age represents the time of glacier retreat, however the differences between these independent chronologies is potentially much larger than anticipated. In this particular study area, neither dating technique is without its challenges; for OSL, these include the small proportion of grains that pass the acceptance criteria, their relatively low signal intensity, the large OD values, and relatively large uncertainties determined for the D_e values, whilst for TCN there is no accurate ^{10}Be production rate for this region, and the ages within a single landform can be very scattered due to complicated geological processes affecting boulders (Owen and Dortch, 2014).

In summary, our OSL ages are consistent with the depositional sequence of events derived from the geomorphology, and also with the radiocarbon ages, but they are more difficult to reconcile with the TCN ages.

5. Conclusions

Five glacial samples collected from moraines outside the Baiyu Valley in southeastern Tibet were dated using a SAR OSL protocol applied to single grains of quartz. Many of these quartz grains demonstrated poor luminescence characteristics and hence failed screening criteria, including the OSL IR depletion ratio test. The age of sample BY203 could not be determined due to insufficient grains passing the screening criteria and hence giving D_e determinations. The single grain OSL ages of the other four samples are consistent with geomorphological relationships and with the radiocarbon ages. It is more difficult to integrate the OSL and TCN data, and it is not clear whether the apparent differences in ages are due to problems in one, or even both of these methods, or because they are dating different events.

Single grain measurements demonstrate that incomplete bleaching is common in these glacial samples prior to deposition, as suggested by the scattered D_e distributions. However, the large overdispersion seen in the dose recovery experiments makes interpretation of this scatter complex. Analysis and interpretation of single grain OSL measurements of quartz from glacial sediments in this area of southeastern Tibet is complex. Further work is required to increase confidence in the veracity of the OSL ages obtained for these materials.

Acknowledgements

This study was supported by the National Natural Sciences Foundation of China (grants 41371080, 41290252, and 41271077), 'Strategic Priority Research Program (B)' of the Chinese Academy of Sciences (XDB03030100) and the State Key Laboratory of Cryospheric Sciences (SKLCS-ZZ-2013-01-05). XJO was an academic visitor at Aberystwyth Luminescence Research Laboratory (ALRL) (October 2013−October 2014) sponsored by the China Scholarship Council. XJO would like to thank Hollie Wynne, Melissa Chapot, Debra Colarossi and Rachel Smedley for their kind help at ALRL.

References

Balco, G., 2011. Contributions and unrealized potential contributions of cosmogenic-nuclide exposure dating to glacier chronology, 1990–2010. Quaternary Science Reviews 30, 3-27.

Chen, R.R., Zhou, S.Z., Lai, Z.P., Ou, X.J., Chen, R., Deng, Y.B., 2014. Luminescence chronology of late Quaternary moraines and Last Glacial Maximum equilibrium-line altitude reconstruction from Parlung Zangbo Valley, south-eastern Tibetan Plateau. Journal of Quaternary Science 29, 597-604.

Chmeleff, J., von Blanckenburg, F., Kossert, K., Jakob, D., 2010. Determination of the 10Be half-life by multicollector ICP-MS and liquid scintillation counting. Nuclear Instruments and Methods in Physics Research Section B: Beam Interactions with Materials and Atoms 268, 192-199.

Duller, G.A.T., 2003. Distinguishing quartz and feldspar in single grain luminescence measurements. Radiation Measurements 37, 161-165.

Duller, G.A.T., 2006. Single grain optical dating of glacigenic deposits. Quaternary Geochronology 1, 296-304.

Duller, G.A.T., 2008. Single-grain optical dating of Quaternary sediments: why aliquot size matters in luminescence dating. Boreas 37, 589-612.

Galbraith, R.F., Roberts, R.G., Laslett, G., Yoshida, H., Olley, J.M., 1999. Optical dating of single and multiple grains of quartz from Jinmium Rock Shelter, northern Australia: part I, experimental design and statistical models. Archaeometry 41, 339-364.

Heyman, J., Stroeven, A.P., Harbor, J.M., Caffee, M.W., 2011. Too young or too old: Evaluating cosmogenic exposure dating based on an analysis of compiled boulder exposure ages. Earth and Planetary Science Letters 302, 71-80.

Hu, G., Yi, C.-L., Zhang, J.-F., Liu, J.-H., Jiang, T., Qin, X., 2014. Optically stimulated luminescence dating of a moraine and a terrace in Laohugou valley, western Qilian Shan, northeastern Tibet. Quaternary International 321, 37-49.

Korschinek, G., Bergmaier, A., Faestermann, T., Gerstmann, U., Knie, K., Rugel, G., Wallner, A., Dillmann, I., Dollinger, G., Von Gostomski, C.L., 2010. A new value for the half-life of 10Be by Heavy-Ion Elastic Recoil Detection and liquid scintillation counting. Nuclear Instruments and Methods in Physics Research Section B: Beam Interactions with Materials and Atoms 268, 187-191.

Lal, D., 1991. Cosmic ray labeling of erosion surfaces: in situ nuclide production rates and erosion models. Earth and Planetary Science Letters 104, 424-439.

Li, J.J., Zheng, B.X., Yang, X.J., Xie, Y.Q., Zhang, L.Y., Ma, Z.H., Xu, S.Y., 1986. Glaciers in Tibet (in Chinese with English abstract). Science Press, Beijing.

Murray, A.S., Wintle, A.G., 2000. Luminescence dating of quartz using an improved single-aliquot regenerative-dose protocol. Radiation Measurements 32, 57-73.

Ou, X.J., Lai, Z.P., Zhou, S.Z., Chen, R., Zeng, L.H., 2015. Optical dating of young glacial sediments from the source area of the Urumqi River in Tianshan Mountians, northwestern China. Quaternary International, in press.

Ou, X.J., Lai, Z.P., Zhou, S.Z., Zeng, L.H., 2014. Timing of glacier fluctuations and trigger mechanisms in eastern Qinghai-Tibetan Plateau during the Late Quaternary. Quaternary Research 81, 464-475.

Owen, L.A., Dortch, J.M., 2014. Nature and timing of Quaternary glaciation in the Himalayan-Tibetan orogen. Quaternary Science Reviews 88, 14-54.

Owen, L.A., Robinson, R., Benn, D.I., Finkel, R.C., Davis, N.K., Yi, C.L., Putkonen, J., Li, D.W., Murray, A.S., 2009. Quaternary glaciation of Mount Everest. Quaternary Science Reviews 28, 1412-1433.

Putkonen, J., Swanson, T., 2003. Accuracy of cosmogenic ages for moraines. Quaternary Research 59, 255-261.

Rhodes, E.J., Bailey, R.M., 1997. The effect of thermal transfer on the zeroing of the luminescence of quartz from recent glaciofluvial sediments. Quaternary Science Reviews 16, 291-298.

Richards, B.W.M., Benn, D.I., Owen, L.A., Rhodes, E.J., Spencer, J.Q., 2000. Timing of late Quaternary glaciations south of Mount Everest in the Khumbu Himal, Nepal. Geological Society of America Bulletin 112, 1621-1632.

Spencer, J.Q., Owen, L.A., 2004. Optically stimulated luminescence dating of Late Quaternary glaciogenic sediments in the upper Hunza valley: validating the timing of glaciation and assessing dating methods. Quaternary Science Reviews 23, 175-191.

Stone, J.O., 2000. Air pressure and cosmogenic isotope production. Journal of Geophysical Research: Solid Earth (1978–2012) 105, 23753-23759.

Tsukamoto, S., Asahi, K., Watanabe, T., Rink, W.J., 2002. Timing of past glaciations in Kanchenjunga Himal, Nepal by optically stimulated luminescence dating of tills. Quaternary International 97-98, 57-67.

Xu, X., Yang, J., Dong, G., Wang, L., Miller, L., 2009. OSL dating of glacier extent during the Last Glacial and the Kanas Lake basin formation in Kanas River valley, Altai Mountains, China. Geomorphology 112, 306-317.

Zhang, B., Ou, X.J., Lai, Z.P., 2012. OSL ages revealing the glacier retreat in the Dangzi valley in the eastern Tibetan Plateau during the Last Glacial Maximum. Quaternary Geochronology 10, 244-249.

Zhao, J.D., Lai, Z.P., Liu, S.Y., Song, Y.G., Li, Z.Q., Yin, X.F., 2012. OSL and ESR dating of glacial deposits and its implications for glacial landform evolution in the Bogeda Peak area, Tianshan range, china. Quaternary Geochronology 10, 237-243.

Zhou, S.Z., Wang, J., Xu, L.B., Wang, X.L., Colgan, P.M., Mickelson, D.M., 2010. Glacial advances in southeastern Tibet during late Quaternary and their implications for climatic changes. Quaternary International 218, 58-66.

Zhou, S.Z., Xu, L.B., Colgan, P.M., Mickelson, D.M., Wang, X.L., Wang, J., Zhong, W., 2007. Cosmogenic Be-10 dating of Guxiang and Baiyu glaciations. Chinese Science Bulletin 52, 1387-1393.

Table

Table 1: Sample information, equivalent dose (D_e) values, and OSL ages determined for samples from Baiyu Valley (Aberystwyth Luminescence Research Laboratory sample code prefix: Aber/213/BY). D_e values were determined using both the central age model (CAM) and minimum age model (MAM). Ages were calculated to 3 significant figures using the dose rate values given in Table S1 (prior to rounding), and are only shown for the model viewed as the most appropriate for determination of D_e. Ages refer to a datum of A.D. 2010. No age was determined for sample BY203.

Sample No.	Sedimentary deposit	No. grains (accepted / measured)	CAM D_e (Gy)	MAM D_e (Gy)	OD (%)	CAM age (ka)	MAM age (ka)
BY201	Glaciofluvial	49/4500	72.2 ± 10.5	24.3 ± 6.9	93.0 ± 1.6	-	**9.43 ± 2.72**
BY202	Till	62/4500	56.2 ± 7.5	21.9 ± 6.7	92.6 ± 1.4	-	**7.95 ± 2.47**
BY203	Till	9/3800	35.8 ± 11.1	17.0 ± 14.6	73.4 ± 9.3	-	-
BY301	Till	71/3700	54.3 ± 5.6	39.3 ± 11.4	75.5 ± 1.0	-	**14.4 ± 4.2**
BY302	Glaciofluvial	96/2100	48.5 ± 3.4	29.7 ± 12.1	54.5 ± 0.6	**11.3 ± 1.0**	-

Figure Captions

Figure 1: Map of the study area, showing glacial landforms and sampling sites. Google Earth images showing (a) location of the study area in southeastern Tibet, and (b) the Bodui Zangbo River and Parlung Zangbo River; the rectangle indicates the area shown in (c). Fig. (c) shows the glacial landforms at the mouth of the Baiyu Valley, the OSL sampling sites, and independent terrestrial cosmogenic nuclide (TCN) ages (in ka) and radiocarbon (^{14}C) ages (in cal ka BP) (Zhou et al., 2010). Arrows indicate the direction of modern river flow. Photographs of the sections sampled are also shown, adjacent to their respective landforms.

Figure 2: (a, b) Typical dose response curve, and (inset) OSL decay curve, from two single grains analysed in the dose recovery test. The grain shown in (a) is typical of those grains which exhibit a bright OSL signal, but which fail the OSL IR depletion ratio test (0.14 ± 0.02); (b) shows an example of a grain which passes the OSL IR test (0.85 ± 0.30). These tend to be relatively dim. (c) Dose recovery data for 34 grains which passed all acceptance criteria. The grey band indicates the given dose (68.8 Gy), and the solid line indicates the recovered dose.

Figure 3: Radial plots showing the natural D_e distribution of (a) BY202 which has an OD that is typical of most of the samples. The grey band is the D_e calculated using the MAM. (b) Data for BY302 which has a lower OD and whose D_e has been calculated using the CAM.

Published in Quaternary Geochronology (2015) – DOI: 10.1016/j.quageo.2015.02.018

Fig. 1

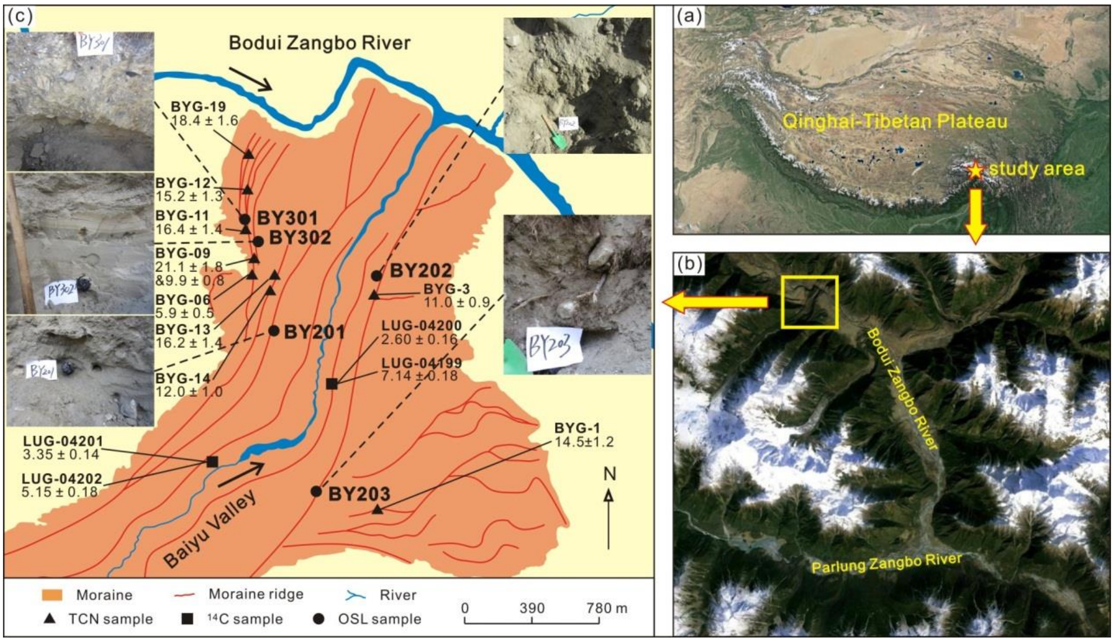

Published in Quaternary Geochronology (2015) – DOI: 10.1016/j.quageo.2015.02.018

Fig. 2

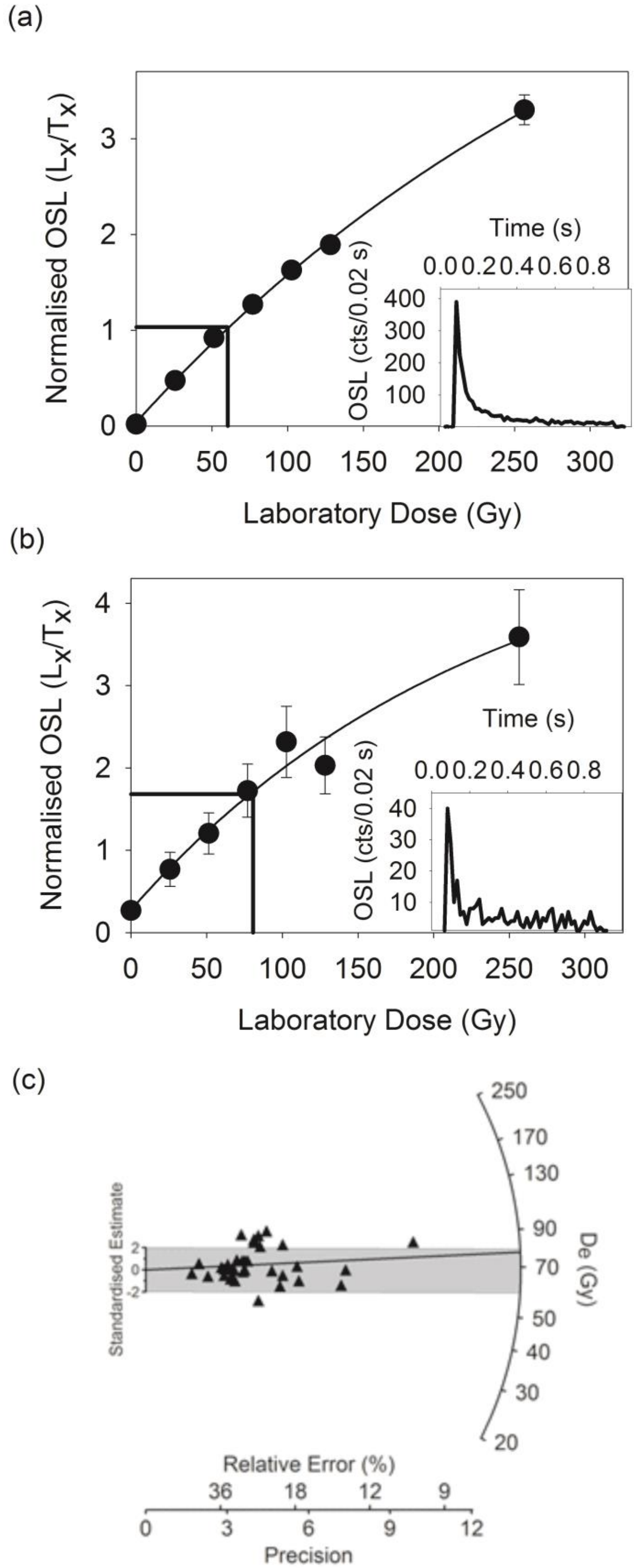

Fig. 3

(a) BY202

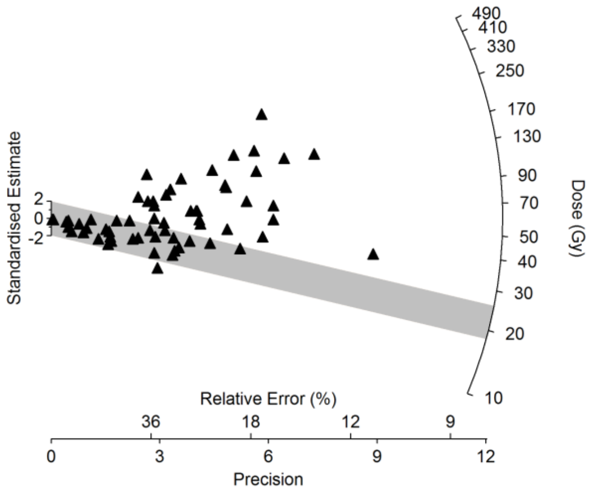

(b) BY302